Cerâmica. 2024, v.70:eFIUE4889
**ORIGINAL ARTICLE**
http://dx.doi.org/10.1590/FIUE4889

# Temperature-Dependent Evolution and Characterization of Heat-Treated Palygorskite Clay Mineral

*Thonny Su Chen[1], Thais Ferreira da Silva[2*], Ana Paula Fonseca Albers[1], Eduardo Quinteiro[1], Fabio Roberto Passador[2].*
*[1]Federal University of São Paulo (UNIFESP), Ceramic Technology Laboratory, 330 Talim St., São José dos Campos, SP, Brazil, 12231-280.*
*[2]Federal University of São Paulo (UNIFESP), Polymer and Biopolymer Technology Laboratory (TecPBio), 330 Talim St., São José dos Campos, SP, Brazil, 12231-280.*

**Abstract**

Depending on the geological origin, Palygorskite (Pal) is associated with the presence of several accessory minerals and organic matter that need to be removed so as not to interfere with its final application. In this way, the purification of raw Pal was carried out through heat treatment. The raw Pal samples were subjected to heat treatment at 100 °C, 300 °C, 500 °C, 700 °C, 800 °C, and 900 °C for 4 hours using a muffle furnace. The samples were characterized by X-ray fluorescence spectrometry (XRF), X-ray diffraction (XRD), thermogravimetric analysis (TGA), physisorption employing the B.E.T method, and field emission gun scanning electron microscopy (FEG-SEM). After the purification process by heat treatment, the reduction of quartz, calcite, dolomite, and kaolinite was observed. The results of the purification process of raw Pal using heat treatment are promising, fast, low-cost, environmentally friendly, and high-yield, and can replace the chemical treatments usually used.
**Keywords**: Palygorskite; heat treatment; heat-activated; purification process; low-cost process.

## INTRODUCTION

Palygorskite (Pal) is a hydrated clay mineral primarily composed of silicon, magnesium, aluminum, and oxygen, characterized by its microfibrous morphology, high surface area, and low surface charges [1]. Its structure composition was initially studied by Bradley [2] in 1940, yielding the theoretical formula of $Si_8O_{20}Mg_5(Al)(OH)_2(H_2O)_4 \cdot 4H_2O$. Pal is a fibrous clay mineral, featuring a 2:1 phyllosilicate strand bonded by apical oxygen inversion in the continuous tetrahedral sheet, occurring every four Si atoms [3,4,5]. In contrast to planar phyllosilicates like montmorillonite and mica, fibrous clays consist of two-dimensional tetrahedral sheets and discrete octahedral sheets, giving rise to parallel structural tunnels/channels along the clay fibers [3,6]. The dimensions of the zeolite channels in Pal measure 6.4 Å x 3.7 Å [3,7] as shown in Figure 1.

Due to its large specific surface area, natural nano-sized zeolite pores, and many activation sites, Pal is showing excellent filling performance and has become a good polymer carrier, for example. It is easily dryable, non-toxic, tastes, less, and is of low hardness. These characteristics make it superior to other inorganic fillers for the modification of polymers [8, 9].

The geological formation of the Pal favors the presence of several accessory minerals (mica, quartz, dolomite, and calcite, among others, in addition to the presence of organic matter). Depending on the desired application, it is necessary to separate the main clay mineral from the impurities (organic matter and accessory minerals), this process is called purification. The purification of raw Pal can be carried out in several ways, among them, it is possible chemical treatments and heat treatments.

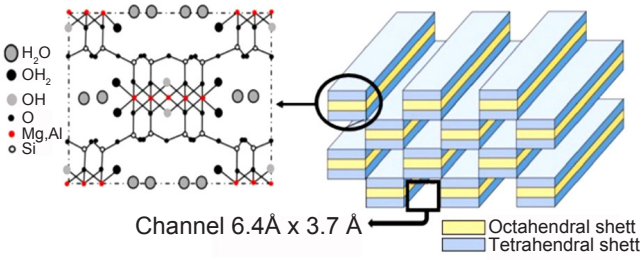


Figure 1: Scheme of morphology and chemical structure of Pal.

When acids are employed in the chemical treatment, this process is generally referred to as acid activation. Acids such as hydrochloric acid (HCl), sulfuric acid ($H_2SO_4$), and nitric acid ($HNO_3$) are commonly used for these treatments. This type of treatment increases the surface area, porosity, and acidity of the clay surface [10,11, 12, 13].

In our previous work [11] a comparative study of processes for purification and acid activation of Pal was carried out, in this study, two processes (milling and sonication) and two dispersing agents (sodium polyacrylate and sodium silicate) were tested. As a result, it was found

* *thais.ferret@hotmail.com*
*https://orcid.org/0000-0002-2022-5050*

that the best methodology to achieve the highest efficiency in Pal purification was the association of the sonication mixing process and the use of sodium polyacrylate as a dispersing agent, followed by activation with hydrogen peroxide and sulfuric acid. This process did not change the fibrous morphology after the Pal purification steps and increased its Pal surface area.

Several studies have investigated the purification of Pal under various conditions. Barrios *et al.* [14] treated Pal with acid concentrations ranging from 1 to 7 M HCl for 1 hour at room temperature. The clay treated in 7 M HCl underwent leaching, while treatment with 5 M HCl yielded the best results, maintaining the crystalline structure of the clay and increasing the surface area to 280 m²/g. Neto *et al.* [15] used Pal from different deposits in Guadalupe, Brazil, activating it in solutions of 1 to 7 M HCl at 70°C for periods ranging from 0.5 to 7 hours. The optimal result was observed for clay treated with 7 M HCl for 7 hours, which showed no structural changes and achieved surface areas above 200 m²/g. They also reduced the quartz content through a pre-hydration and scrubbing process, meeting the specifications for pharmaceutical use. Boudriche *et al.* [16] activated Pal with HCl at concentrations of 0.5, 1, 3, and 5 M. They found that at low HCl concentrations (≤1 M), the morphology and crystalline structure of Pal were preserved, and carbonate dissolution occurred.

In heat treatments, the objective is to modify the structure and composition of the clay through controlled heating or cooling. This process results in the removal of organic matter, adsorbed water, and hydroxyls present in the structure, consequently increasing its surface area [10].

Sepiolite is another fibrous clay with a mineralogical structure very similar to Pal, their purification processes are very close as well. During the heat treatment, Pal and sepiolite exhibit four distinct temperature ranges, each associated with dehydration processes and changes in porosity. The specific temperature ranges can vary widely based on factors such as the thermal treatment protocol, prior processing, and the geological origin of the clay under study. These factors impact the chemical composition (including the number of isomorphic substitutions), the presence of accessory minerals, and the overall structure of the clay minerals [10,11].

In the first stage of dehydration, the zeolite water and the water adsorbed on the outer surface of the clay are lost at temperatures below 200 °C [17,18]. Subsequently, in the second stage, approximately half of the coordination water is lost, leading to the partial collapse of the clay structure and a fold of its lattice, occurring around 300-380 °C in sepiolite and between 200-280 °C in Pal [10,17]. In the third stage, all coordination water and a portion of the structural water are removed, accompanied by the elimination of hydroxyls linked to $Fe^{3+}$ and $Al^{3+}$ ions in the octahedral sheet. This occurs within the temperature range between 380-680 °C in sepiolite and between 280-580 °C in Pal [10,17,18]. Finally, in the fourth stage, all structural water is eliminated, resulting in the loss of hydroxyls linked to the $Mg^{2+}$ ion in the octahedral sheet [17,19,20]. The resulting crystalline phase is enstatite, formed at temperatures above 800 °C following the complete dehydroxylation of clays [19,21,22].

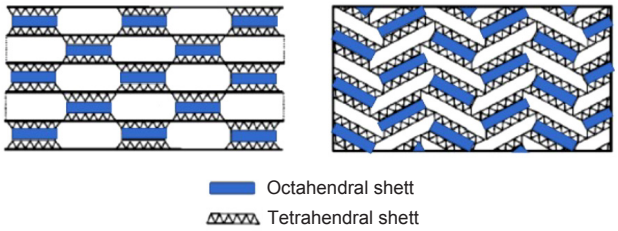


Figure 2: Simplified diagram of the structure of fibrous clays (A) before and (B) after the bending suffered by the loss of coordination water.

The silanol groups in sepiolite have high thermal stability and do not undergo dehydroxylation by heat treatments at temperatures below 1100 °C; in the case of Pal, the thermal stability should remain like that presented by sepiolite [23]. Figure 2 shows the structure of the Pal after the elimination of the first two coordinated water molecules.

The presence of defects is common in the structure of fibrous clays, Krekeler and Guggenheim [24], using transmission electron microscopy (TEM), observed three main types of defects in Palygorskite–sepiolite. These include the omission of sets of octahedral and tetrahedral sheets in the form of the 2:1 structure, resulting in the creation of open channel defects (OCD) and thereby opening the internal channels of the fibrous clay. Additionally, there are planar defects and stacking defects in the formation of the structure. These defects are among the factors contributing to variations in the properties of fibrous clays from different regions. They account for differences in water content, the quantity of stabilizing cations, and the presence of organic matter within the clay channels. These variations directly impact the time and temperature required for heat treatment [9]. Yan *et al.* [20] noted that most of the Pal hydroxyls are lost at temperatures below 450 °C and complete dehydroxylation occurs close to 700 °C, in addition, at temperatures above 900 °C there is a drastic change in the crystalline structure of clay.

When all the coordination water is eliminated, the clay transforms into its anhydride state and loses its hygroscopic ability. Consequently, rehydration of Pal can only occur if it has been treated at low temperatures. Kuang *et al.* [25] conducting rehydration treatments on clays heat treated at 150 °C and 300 °C, found through -nuclear magnetic resonance that clays treated at these temperatures rehydrated when exposed to water vapor. This process allows them to regain the structure lost with the removal of zeolitic water.

Furthermore, there is also the possibility of combining chemical and thermal treatments. Through the combination of acid activation and heat treatment of sepiolite, Balci [26] observed that conducting the acid activation and heat treatment led to the removal of a portion of the adsorbed water and zeolite water before the final treatment. Additionally, acid activation limited crystalline deformation during heat

treatment due to the formation of pores through the leaching of $Mg^{2+}$ ions. This prevented the merging of micropores and the collapse of the structure. Pal likely experiences a similar effect from the combined treatments due to the similarity of their structures.

The Pal purification process by chemical treatments is one of the most used, generally involving acid activation, which produces a large modification of the surface area, increasing the number of acid sites [1,12,14]. As a disadvantage, acid activation generates chemical residue during clay washing to remove post-treatment acidity. Furthermore, the use of strong acids for the purification process is not a sustainable and environmentally promising alternative.

In the case of thermal activation, the modification of the structure occurs through the elimination of water molecules present in the clay or adsorbed on its surface. Furthermore, processes of decomposition of minerals such as carbonates and volatilization of organic compounds may end up occurring simultaneously with the dehydration process. Thermal activation can also produce an increase in acidic sites in the clay, through the exposure of ions in the structure, as water molecules are eliminated [10]. As an advantage of thermal activation, there is no need to use external reagents, such as acid, eliminating the need for washing post-treatment clay, thus not generating chemical residues. The potential for modifying the properties of clays through thermal activation is still being investigated, and it is important to expand studies in this area.

In this work, an easy, fast, and low-cost process is being proposed for the purification of raw Pal. The heat treatment was carried out in a muffle furnace at different temperatures, maintaining the same time. The evaluation of the evolution of the purification process was carried out using different techniques, making it possible to determine the appropriate temperature for purifying raw Pal.

## EXPERIMENTAL

Raw Palygorskite (Pal) was supplied by Brazil Minas (Brazil), with specification BRM F 14-EPA 13.04, with a density ranging from 2.00 to 2.25 g/cm$^3$, and a retention of < 10 wt% on 325 mesh sieves (with a nominal opening of 45 μm).

The raw Pal used in this work was pre-sieved to 325 mesh. The raw Pal (Pal(raw)) was heat treated in a muffle furnace at temperatures of 100 °C, 300 °C, 500 °C, 700 °C, 800 °C, and 900 °C for 4 hours with a heating rate of 10 °C/min. The heat-treated samples were named Pal(100), Pal(300), Pal(500), Pal(700), Pal(800), and Pal(900) according to the temperature used in the heat treatment.

The chemical composition of the samples was analyzed using X-ray fluorescence (XRF) analysis using a Zetium spectrometer (Malvern Panalytical). The samples were fused with lithium tetraborate, and the calibration ROC-1 (Rocks) was applied. Loss on ignition (LOI) was conducted at 1020 °C for 2 h.

To identify the crystalline phases, an X-ray diffractometer (Ultima IV, Rigaku) was used, with CuKα radiation (λ=1.54056 Å). The equipment operated at a scanning rate of 0.2 °/s with a 2θ range from 5° to 55°. The interlayer spacing (d) was determined using Bragg's equation ($2d.\sin\theta = n.\lambda$).

The thermal stability was evaluated by thermogravimetric analysis (TGA) using TA Instruments, model Q50, from room temperature to 800 °C, with a heating rate of 20 °C/min under a constant nitrogen flow of 20 mL.min$^{-1}$.

The surface area was determined through the analysis of $N_2$ adsorption using the B.E.T. method. The tests were performed with a gas sorption analyzer (Nova 4200e, Quantachrome Instr.). The samples were heated to 100 °C and degassed for 4 hours.

The morphology of Pal(raw) was characterized by a transmission electron microscope (TEM). For the TEM sample, Pal(raw) powder was mixed in acetone, followed by ultrasonication. A drop of the solution was added to the TEM sample holder and the analysis was performed after solvent evaporation. A TEM micrograph of Pal(raw) was obtained using an FEI Eagle Camera attached to the Tecnai F20 microscope at 200 keV operating voltage.

The morphologies and particle size measurements of the heat-treated Pal samples were evaluated on a TESCAN-MIRA3 field-emission gun scanning electron microscope operating at 10 kV. For the analysis, the heat-treated Pal powder was affixed onto a conductive carbon tape and covered with a thin gold layer before imaging.

## RESULTS AND DISCUSSION

After the heat treatments, noticeable resulting color differences were observed between the samples, as shown in Figure 3. It is evident that as the temperature of the heat treatment increases, there is a gradual deepening of the shade of clay. This color change is commonly attributed to water loss, the thermal decomposition of compounds present in the clay, such as kaolinite, calcite, and dolomite, and mainly due to the iron ion typically present in the mineral clay structure or as accessory minerals (ilmenite and hematite).

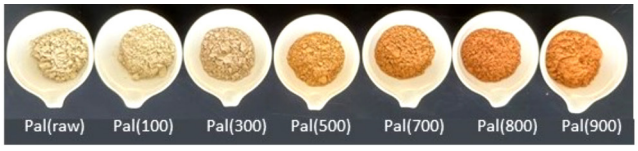


Figure 3: The visual appearance of Pal after heat treatments.

Table I presents the percentage ratio of oxides found in each of the heat-treated Pal samples. The main oxides present in the samples are $SiO_2$, $Al_2O_3$, $Fe_2O_3$, CaO, MgO, and $K_2O$. $SiO_2$ and $Al_2O_3$ probably originate from the composition of Pal, along with other clay minerals in smaller proportions. The presence of a fraction of $Fe_2O_3$ and MgO can be attributed to isomorphic substitutions occurring mainly in the octahedral sheet of clay minerals, involving $Fe^{3+}$ and $Mg^{2+}$ ions, in addition to fractions that may be present as accessory minerals. The contents of MnO, $K_2O$,

Table I. Relationship of oxides present in raw Pal and heat-treated Pal (% mass).

| | Pal (raw) | Pal (100) 100 °C | Pal (300) 300 °C | Pal (500) 500 °C | Pal (700) 700 °C | Pal (800) 800 °C | Pal (900) 900 °C |
|---|---|---|---|---|---|---|---|
| $SiO_2$ (%) | 50.80 | 52.60 | 53.20 | 55.60 | 57.40 | 59.50 | 60.80 |
| $Al_2O_3$ (%) | 11.80 | 11.20 | 11.40 | 11.90 | 12.30 | 12.70 | 13.00 |
| $Fe_2O_3$ (%) | 5.95 | 5.53 | 5.59 | 5.81 | 6.00 | 6.18 | 6.39 |
| MnO (%) | 0.42 | 0.41 | 0.42 | 0.44 | 0.45 | 0.47 | 0.48 |
| MgO (%) | 4.47 | 4.24 | 4.37 | 4.57 | 4.70 | 4.84 | 4.94 |
| CaO (%) | 8.56 | 7.10 | 7.40 | 7.65 | 7.96 | 8.25 | 8.49 |
| $Na_2O$ (%) | <0.10 | <0.10 | <0.10 | 0.10 | 0.10 | <0.10 | 0.11 |
| $K_2O$ (%) | 2.12 | 1.97 | 2.02 | 2.09 | 2.18 | 2.23 | 2.30 |
| $TiO_2$ (%) | 0.54 | 0.51 | 0.52 | 0.54 | 0.55 | 0.57 | 0.59 |
| $P_2O_5$ (%) | <0.10 | <0.10 | <0.10 | <0.10 | <0.10 | <0.10 | <0.10 |
| LOI* (%) | 15.0 | 15.60 | 14.0 | 10.70 | 7.99 | 4.26 | 1.93 |

**LOI=loss on ignition (1020°C)*

and $TiO_2$ must be exclusively associated with the presence of accessory minerals. CaO and fraction of the MgO-like stem from accessory minerals.

It is noteworthy that there is an increase in the percentage of all oxides with the rise in heat treatment temperature applied to the clays. This rise in percentage can be attributed to the removal of adsorbed water, zeolite water, coordination water, structural water, and gases resulting from possible chemical reactions involving mass loss.

In our previous study [11] with acid purification, it was possible to confirm the significant reduction of the calcite content due to acid activation (from 8.56% to about 1% CaO) and a slight increase in the contents of $Al_2O_3$ and $Fe_2O_3$, which were also present in the Pal composition (both Al and Fe can make isomorphic substitutions with Mg).

Figure 4 shows the loss of ignition values measured by XRF after calcination at 1020 °C of raw Pal and heat-treated Pal at various temperatures. A consistent decrease in loss on ignition is observed across the heat-treated clays. As the heat treatment temperature increases, the rate of loss on ignition tends to be lower in comparison to Pal heat-treated at lower temperatures, suggesting the occurrence of irreversible reactions. The most significant rate of loss on ignition was observed after heat treatment at 500 °C. This fact is associated with the presence of multiple reactions of clay mineral structural transformation and the decomposition of carbonates.

Exanimating diffractograms of the raw Pal and heat-treated Pal it is possible to observe distinct peaks representing Pal, kaolinite, dolomite, calcite, and quartz. The main diffraction peaks for palygorskite occurred at approximately 8.6° (10.27 Å), 19.9° (4.46 Å), and 20.9° (4.25 Å); for calcite, the most significant peak appeared around 29.4° (3.03 Å), while for quartz, it was found at 26.7° (3.34 Å). Additionally, overlapping peaks are also noticeable, particularly in the 2θ range between 35 and 50°. These crystalline phases corroborate the presence of oxides in the chemical analysis (Table 1) and these results are consistent with prior literature [11-13, 26].

According to Bradley [2], the Pal theoretical formula is $Si_8O_{20}Mg_5(Al)(OH)_2(H_2O)_4 \bullet 4H_2O$, in which $Al^{3+}$ ions substitute $Mg^{2+}$ in octahedral sheets. Furthermore, it is possible that $Al^{3+}$ substitutes the $Si^{4+}$ ion in the tetrahedral structure; similarly, ions $Fe^{2+}$ substitute $Mg^{2+}$ in the octahedral sites. Cations such as $K^+$, $Na^+$, or $Ca^{2+}$ normally are present to ensure a balanced charge in clay minerals. These substitutions are fundamental in determining the chemical and physical properties of clay minerals. In this sense, $SiO_2$

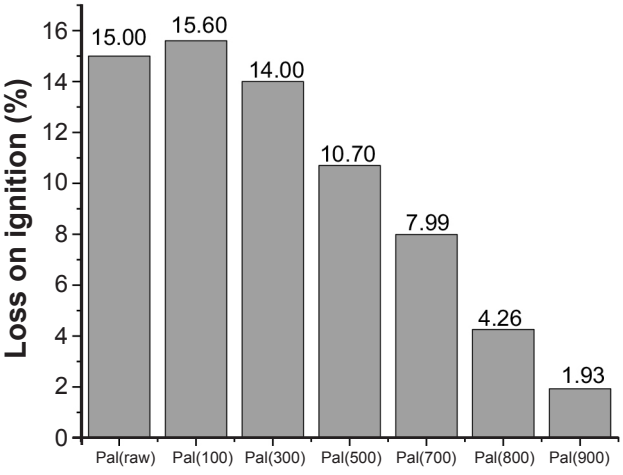


Figure 4: Loss on ignition of heat-treated clays at 1020 °C.

present in Table 1, is sourced from palygorskite, kaolinite ($Al_2Si_2O_5(OH)_4$), and quartz; $Al_2O_3$ from palygorskite and kaolinite mostly; $Fe_2O_3$ mainly from isomorphic substitution in clay minerals, since there were not identified iron-based minerals at the diffractogram (Figure 5). The main fraction of CaO is attributed to calcite, and in a minor amount from dolomite (less intense peak). Based on rational analysis, the estimated amount of palygorskite in natural clay (Pal(raw)) is 19%, calcite around 15%, and quartz 55%; the remainder is related to other minerals, such as kaolinite and dolomite. Figure 5 shows a focused diffractogram within the 2θ range of 6 to 31°, providing a clearer view of the variation in peak intensity. Notably, there is a reduction in the characteristic peak (110) of the raw Pal (Pal(raw)) at 8.5°, nearly disappearing in the Pal(900). This indicates that Pal underwent a structural transformation through the heat treatments, eventually losing nearly all of its structure when treated at 900 °C.

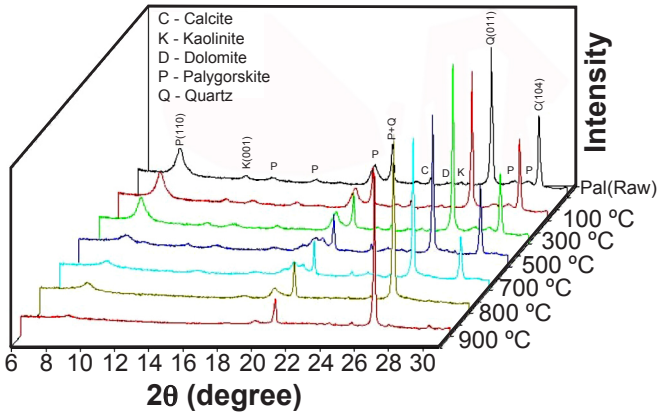


Figure 5: The diffractogram of raw Pal and heat-treated Pal with 2θ ranging from 6° to 31°.

Figure 5 illustrates that the characteristic peak (001) of kaolinite at 12.3° disappears in the sample Pal(700), indicating the decomposition of kaolinite within the temperature range of 500 °C to 700 °C. According to the literature [27], kaolinite dehydration typically occurs between 200 °C and 500 °C, resulting in the transformation into metakaolinite, and the loss of two water molecules, as represented in reaction (A).

$$Al_2Si_2O_5(OH)_4 \rightarrow Al_2Si_2O_7 + 2H_2O \quad (A)$$

The reduction of the calcite peak (104) at 29.5° in the Pal(700) sample also indicates that its calcination process started at a temperature above that of the clay heat-treated at 500 °C. The calcination process was completed during the heat treatment at 800 °C, where the characteristic peak (104) was no longer discernible. This suggests that the calcination process occurred within a temperature range of 500 to 800 °C. This result corroborates the result of the loss on ignition, as depicted in Figure 4. According to the literature [28], the calcination of calcite initiates at temperatures around 700 °C and reaches completion close to 800 °C, although the geological genesis of the mineral and consequently its degree of crystallinity, may affect this decomposition temperature range. In this process, calcium oxide is generated while carbon dioxide is released. The calcination reaction is represented in reaction (B).

$$CaCO_3 \rightarrow CaO + CO_2 \quad (B)$$

In the case of dolomite, the peaks present in the diffractograms were relatively faint, making it difficult to notice them. The dolomite peak disappeared in the sample Pal(800), indicating that dolomite likely underwent some decomposition reaction at temperatures below 800 °C. According to the literature [29], the decomposition of dolomite can occur in several steps or as a one-step process (between 650-850 °C, especially for high rates) depending on the processing conditions and the heating rate of the thermogravimetric analysis.

The characteristic peak (011) of quartz at 26.5° exhibited no significant changes in intensity in any of the heat-treated Pal samples. This indicates that quartz remained unaffected by heating up to 900 °C. Consequently, it can be inferred that the majority of the peaks observed in Pal(900) are attributed to quartz, as the peaks of kaolinite, calcite, and dolomite were no longer discernible at this temperature.

It is possible to evaluate in a semi-quantitative way the structural alterations suffered in the structure of the clay, through the calculation of the ratio between the main peaks of the samples, generating a value of relative intensity between them. As the intensity of the quartz peak (011) showed little variation at different treatment temperatures, the main peak of this phase was used as a reference to evaluate the structural change of the other minerals.

Figure 6 shows the relative intensity between the peaks of Pal(110), calcite (104), and quartz (011). A constant decrease in the ratio P/Q (Pal/quartz) is observed between the Pal(100), Pal(300), and Pal(500) samples. This suggests a significant structure change of the Pal occurred during the heat treatments at 300 °C and 500 °C; after that, no significant changes were observed in the P/Q ratio. Additionally, the C/Q ratio for samples treated at 100 °C and 500 °C is very close, highlighting the stability of the calcite and quartz minerals in this temperature range. After 500 °C, the C/Q ratio decreases and reaches a very small value, due to the thermal decomposition of the carbonate and consequently the relative increase in the quartz content.

At a temperature of 300 °C, an inconsistency in the C/Q relationship was observed. It is important to note that a sample used to carry out this heat treatment was obtained from a second batch of commercial clay, and there may be variations in the calcite content of this batch or even in the quartering operation to obtain this sample. As the P/Q ratio is consistent with the other results, it is unlikely that any deviation from the ideal diffraction condition occurred [30].

Figure 7 presents the TGA and DTG curves for Pal(raw) and heat-treated Pal at different temperatures. Figure 7A shows a continuous mass loss for Pal(raw) and Pal heat-treated

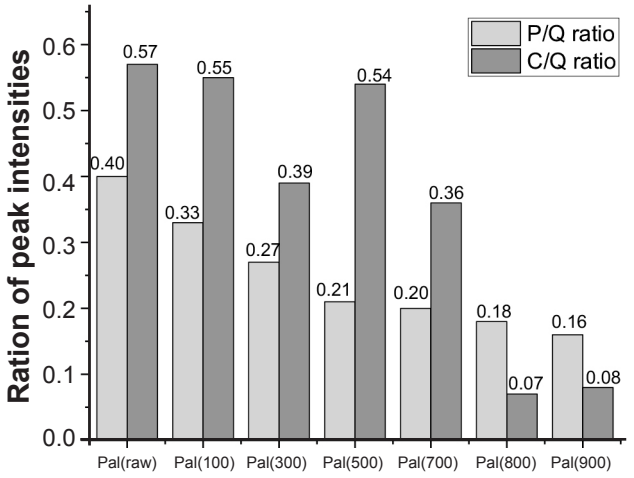


Figure 6:. The ratio of peak intensities between Palygorskite (P), calcite (C), and quartz (Q) peaks.

at 100 °C and 300 °C, it was associated with dehydration and dehydroxylation of Pal, in addition to the decomposition reactions of accessory minerals, such as calcite and dolomite, which release significant amounts of $CO_2$ in the process. For Pal heat treated at 500 °C, 700 °C, and 800 °C, it was observed a significant mass loss after 600 °C (6.86%, 6.38%, and 4.48% respectively), indicating that the main processes of dehydration and dehydroxylation had already occurred and the mass loss after this temperature (600 °C) is related to the decomposition of accessory minerals. Pal heat treated at 900 °C exhibits a very discreet loss mass in all ranges of temperatures. The same behavior of mass variation was also observed in the loss of ignition in Figure 4. These reactions were confirmed by the XRD diffractograms in Figure 5, where the absence of detectable calcite and dolomite peaks in Pal(900) further supports this result.

Figure 7B shows the DTG curves of Pal(raw) and Pal after heat treatment. Four distinct characteristic peaks with significant mass loss are observed. The first peak occurs between 60 °C and 150 °C, corresponding to the loss of adsorbed water and a portion of the zeolite water. The second peak occurred in the range between 180 °C and 240 °C, attributed to the complete removal of zeolite water and partial loss of coordination water. The third peak, ranging from 350 °C to 550 °C, is associated with transforming kaolinite into metakaolinite, the beginning of clay dehydroxylation, and the loss of the last two coordination water molecules. The fourth peak, ranging from 580 °C to 800 °C, corresponds to the end of dehydroxylation and the decomposition of calcite and dolomite. These findings corroborate the results obtained in the XRD analysis (Figure 5) and are consistent with the data presented in Table 2 [19,31].

The final mass loss observed in the thermogravimetry analysis was a bit different from that observed in the loss on ignition obtained in the XRF analysis. It is important to note that the techniques use different amounts of samples to perform the test and this may have affected the results. However, in both analyses, the mass loss values decreased with increasing heat treatment temperature of the clay samples.

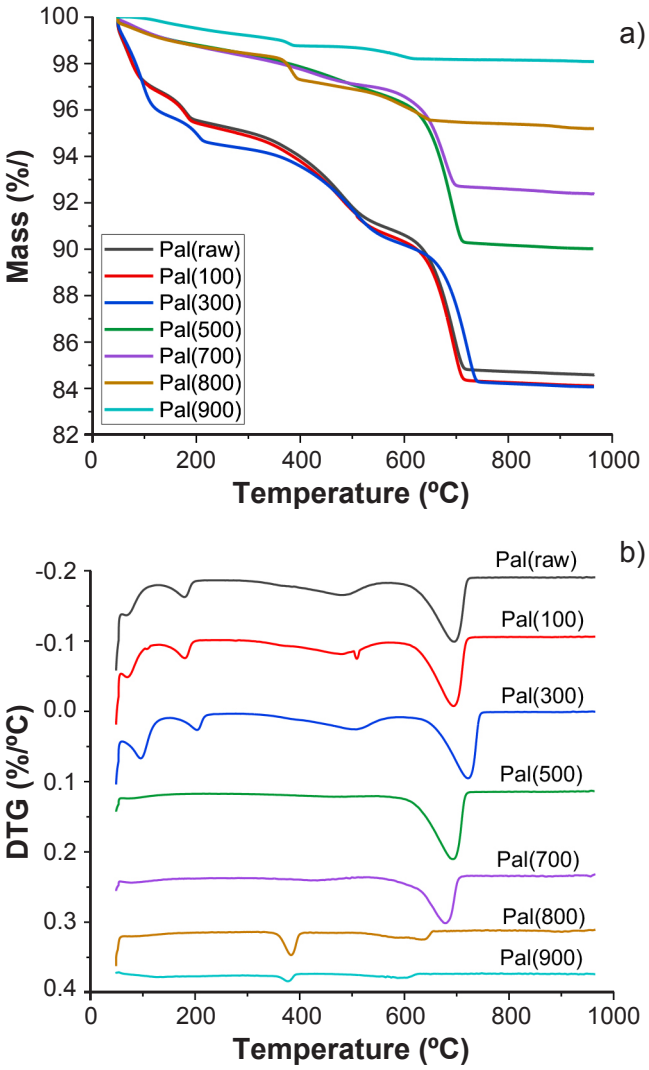


Figure 7. (A) TGA and (B) DTG curves for Pal(raw) and Pal after heat treatment.

Table II shows the mass loss of the samples. The analysis was divided into four temperature ranges that were chosen according to data and literature [11,21,24,32]. Samples Pal(raw), Pal(100), and Pal(300) exhibited considerable mass losses in the temperature range of 60-150 °C, which can be attributed to the hygroscopic property of Pal. However, samples Pal (500), Pal(700), Pal(800), and Pal(900) showed very low mass loss in this temperature range, indicating that above 500 °C the clay lost its hygroscopic capacity.

Pal(100) and Pal(300) exhibited similar mass loss to Pal(raw) in the temperature range of 60-150 °C. This similarity indicates a possible total rehydration of the heat-treated clay, suggesting that there were no significant changes in its structure.

Thermal treatments that eliminate all water coordination led to the transformation of the clay, transforming it into an anhydride state and losing its rehydration capacity [17]. In the case of Pal(700), there was a drastic reduction in mass loss in the temperature ranges of 60-700 °C. This indicates that the clay has been transformed into an anhydride

state. Furthermore, there was a reduction in mass loss in the temperature range above 680 °C, suggesting partial decomposition of calcite and partial dehydroxylation of clay, as there were still significant mass losses in this temperature range.

For the Pal(800) and Pal(900) samples, the loss of hygroscopic capacity observed in the Pal(700) sample was maintained, indicating that during the heat treatments, the calcite decomposition and dehydroxylation processes were completed at temperatures below 800 °C, with no natural means of reversing these processes.

The specific surface area and pore volume of the samples were determined through the adsorption and desorption of nitrogen gas for the heat-treated samples as shown in Table III. The heat treatment modified the surface area of the raw Pal. Pal (raw) has a surface area of around 200 $m^2/g$ and heat treatment reduces significantly this value. It is possible to note that the specific surface area of Pal(100) is quite similar to that of Pal(300). This result suggests that the elimination of zeolite water and part of the coordination water molecules did not cause significant structural alteration in the clay. It further implies that the clay did not undergo a dehydration of coordination water exceeding 50% to 65%, which would result in a bending of its lamellar structure and a reduction in surface area [33].

For Pal(500), a significant reduction in clay surface area is observed. This can be attributed to the extensive elimination of coordination water molecules, likely reaching a critical value that leads to the collapse and bend of the clay structure. The value of 77 $m^2/g$ complements the results observed from XRD analysis (Figure 5), indicating that the structural change seen in Figure 6, specifically the decrease in the P/Q ratio between Pal(300) and Pal(500) samples is a result of the folding of the clay structure [33].

The thermal process decreases the surface area of the PaL, while studies [1,34,35] demonstrate that this value is increased with the acid treatment in which the increase is attributed to the dissolution of carbonates that produces an increase in the related proportions of the palygorskite.

Figure 8 shows the physisorption curves of heat-treated samples. The folding of the structure resulted in a slight increase in the volume of pores larger than 20 nm and a slight reduction in the volume of pores with a smaller size, as is evident in Figure 8A. In Figure 8B, it is possible to observe that the heat treatment at temperatures from 300 °C led to a decrease in the volume of micropores within the size range of 2 to 12 nm. This reduction is a consequence of the partial elimination of the coordination water molecules, which caused the collapse of micropores.

Table III - Specific surface area ($S_{BET}$) and pore volume ($V_{0.95}$) of Pal after heat treatment.

| Sample | $S_{BET}$ ($m^2/g$) | $V_{0.95}$ ($cm^3/g$) |
|---|---|---|
| Pal(raw) | 200 | 0.998 |
| Pal(100) | 149 | 0.200 |
| Pal(300) | 117 | 0.169 |
| Pal(500) | 77 | 0.151 |
| Pal(700) | 65 | 0.142 |
| Pal(800) | 10 | 0.022 |
| Pal(900) | 10 | 0.042 |

The small decrease in surface area observed for Pal(700) suggests that the completion of the process of removing coordination water molecules, as observed in DTG (Figure 7B), did not result in significant structural changes in the clay. Additionally, this fact supports the observation that dehydroxylation, also noted in DTG, was completed in the temperature range between 700 °C and 800 °C. This is evident from the drastic reduction in surface area and pore volume observed in the Pal(800) and Pal(900), which was caused by the collapse of the clay channels [1].

Figure 9 shows (A) FEG-SEM and (B) TEM micrographs of Pal(raw). It is possible to observe a fibrous morphology of rod crystals with lengths between 0.5 and 4 μm (predominantly 1 μm). It is also possible to observe a strong tendency for particles to agglomerate, due to secondary bonds and electrostatic forces between the fibrillar crystals. Darker traces in the morphology showed that the impurities are concentrated at the edges and inside the hollow fibers. The morphology observed for Pal(raw) corroborates other studies [11,32,36,37,38].

Figures 10 and 11 present the micrographs of the heat-treated clays, magnified at 50,000x and 100,000x, respectively. In Figure 10, the needle-like shape of the clays and their distribution in the form of clusters with different needle sizes are noticeable. Between temperatures of 100 °C to 300 °C, no observable changes in the structure of the clays. However, for Pal(500), the folding in the clay structure caused by the partial loss of coordination water leads to a slight shrinkage in the size of the clay's needles [19].

In the micrographs, significant differences between the structures of Pal(500) and Pal(700) samples resulting from the removal of all coordination water were not evident.

Table II - Loss of mass (%) of Pal samples along the thermogravimetric analysis.

| | Pal(raw) | Pal(100) | Pal(300) | Pal(500) | Pal(700) | Pal(800) | Pal(900) |
|---|---|---|---|---|---|---|---|
| 60-150 °C | 3.44 | 3.59 | 4.33 | 0.96 | 1.00 | 1.02 | 0.30 |
| 175-350 °C | 5.35 | 5.58 | 5.96 | 1.83 | 1.96 | 1.73 | 0.97 |
| 350-550 °C | 8.92 | 9.25 | 6.26 | 3.27 | 3.06 | 3.36 | 1.47 |
| >680 °C | 12.33 | 13.12 | 11.47 | 6.86 | 6.38 | 4.48 | 1.82 |
| Total Loss (%) | 15.40 | 15.88 | 15.94 | 9.97 | 7.62 | 4.80 | 1.93 |

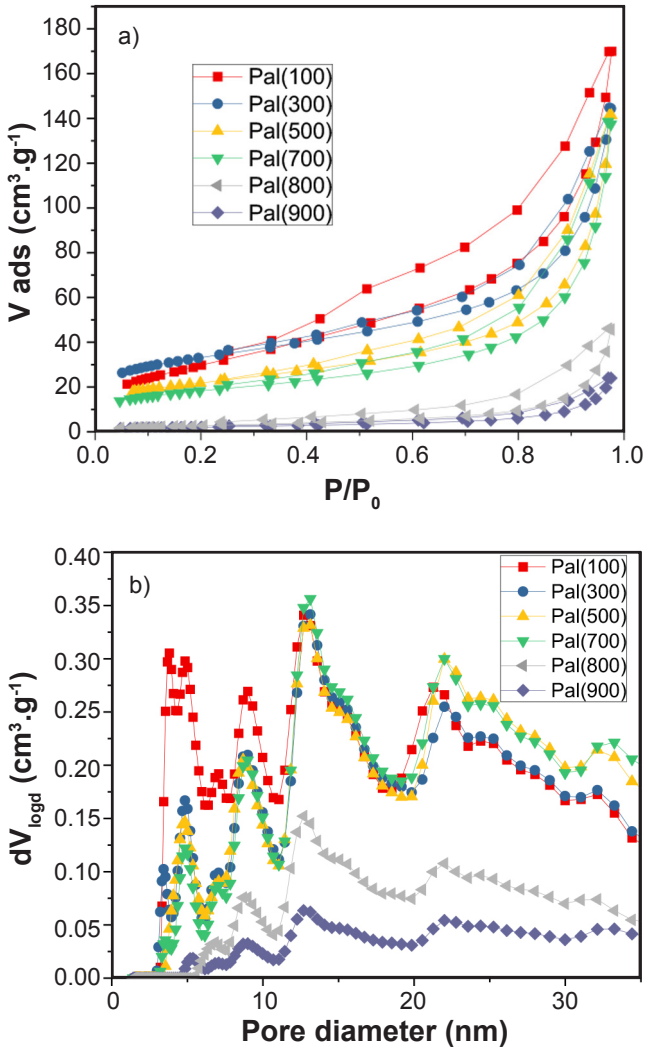


Figure 8: Physisorption curves of heat-treated samples: (A) volume of adsorbed nitrogen gas and (B) pore size distribution.

This aligns with the physisorption analysis which showed little variation in the specific surface area between them, indicating limited structural change.

In the case of Pal(800), the physisorption assay revealed a substantial alteration in its structure. The decrease in clay surface area to 10 $m^2/g$ indicated that processes such as clay dehydroxylation and accessory mineral decomposition led to the collapse of its channels.

In Figure 11 it is possible to observe large distortions in the structure caused by the amorphization and phase transformation of the clay. Both Figures 10 and 11 highlight Pal(900) as the clay undergoing the most significant structural transformation through heat treatment. At this temperature, the clay structure is nearly compacted and subsequent heating post-dehydroxylation may have facilitated the formation of the enstatite crystalline phase. This phase typically emerges at temperatures exceeding 700 °C in Pal and 800 °C in sepiolite [21,22].

Comparing the morphology of the Pal purification processes carried out by chemical treatment and heat treatment [11], it is possible to state that the chemical treatment did not destroy

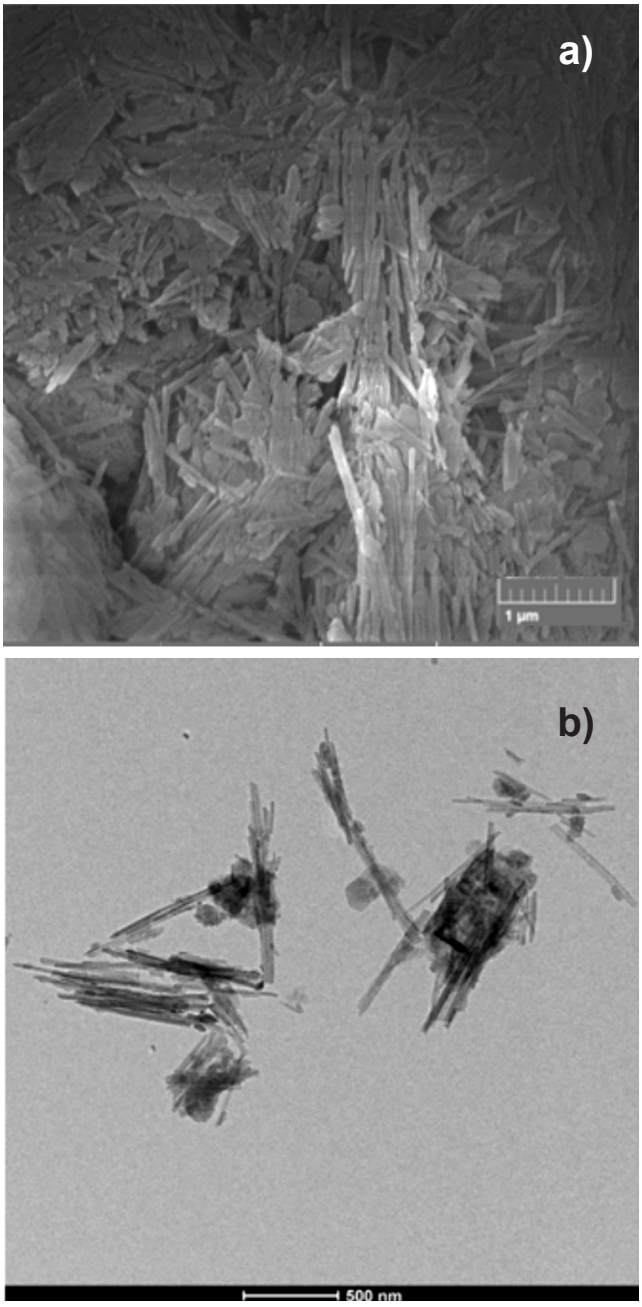


Figure 9: (A) FEG-SEM at 50,000x magnification and (B) TEM micrographs of Pal(raw)

the crystalline structure of Pal [11,32,36,37,38], while at higher temperatures, above 700 °C, there were changes in the crystalline structure as described above.

The chemical treatment increases the surface area and promotes a great reduction of mineral accessories such as calcite, leaching the structure and increasing the adsorption capability of the material as reported by Zhu et al. [39] with the treated clay presented higher toluene adsorption [11, 39]. On the other hand, the heat treatment reduced the surface area of the clay due to the folding process of the structure, but it still can increase the adsorption capability as observed by Chen et al. [40], in which the adsorption capability of ions increases until 700 °C.

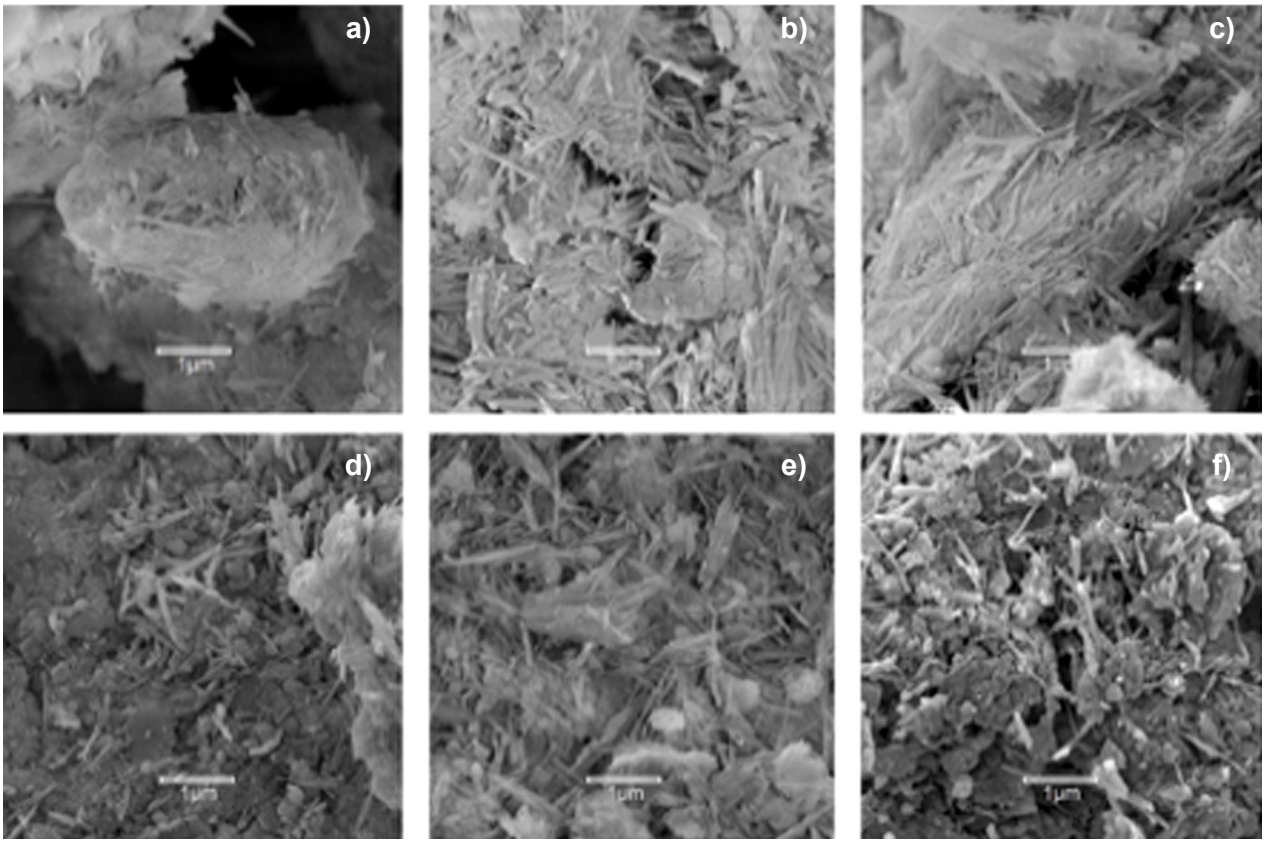


Figure 10: FEG-SEM of heat-treated clays at 50,000x magnification: (A) Pal(100), (B) Pal(300), (C) Pal(500), (D) Pal(700), (E) Pal(800), and (F) Pal(900).

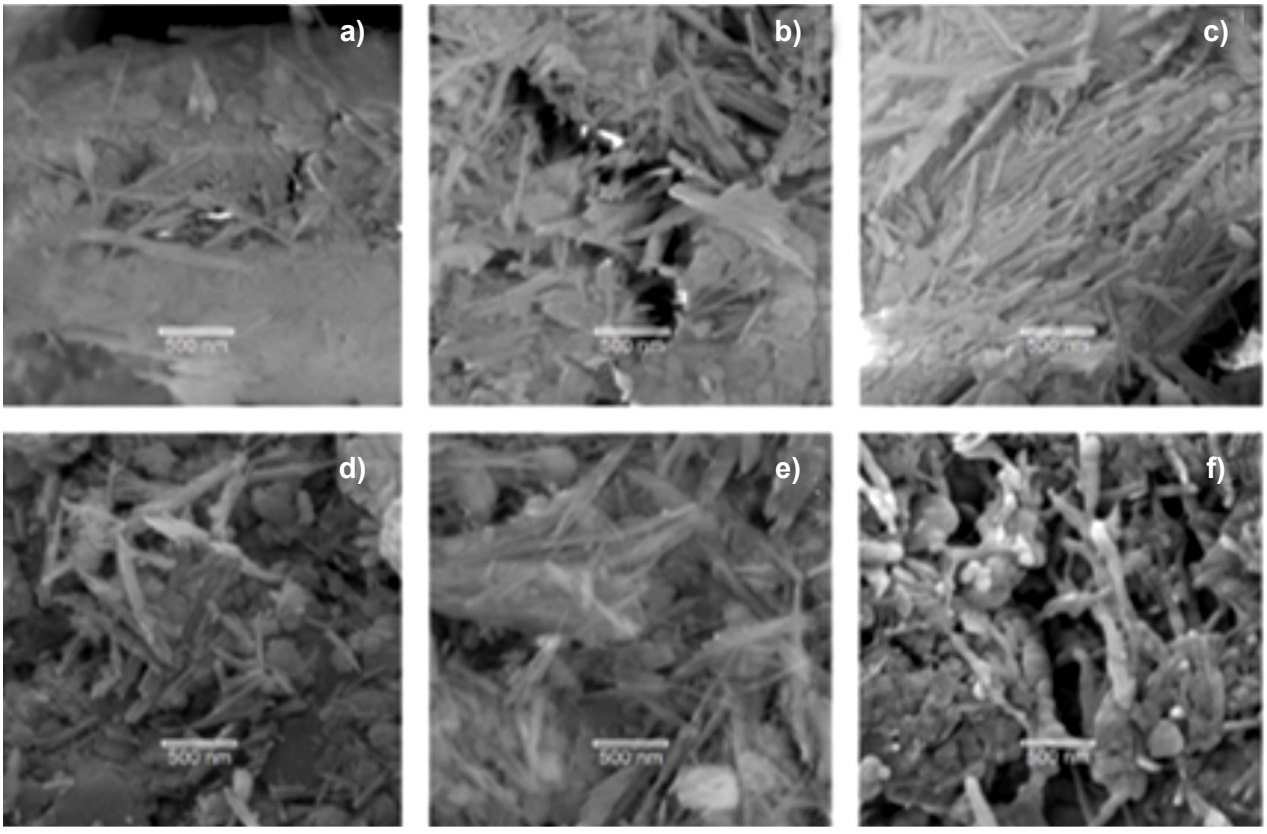


Figure 11: FEG-SEM of heat-treated clays at 10,0000x magnification: (A) Pal(100), (B) Pal(300), (C) Pal(500), (D) Pal(700), (E) Pal(800), and (F) Pal(900).

Taking into account that the surface area is quite important for the adsorption of substances, although acid activation has better performance than thermal activation, it is important to remember that the heat treatment process does not generate waste, which is a great justification for its use. Furthermore, it is an environmentally friendly process, without the generation of solvents, low cost, and high yield, and is very promising for obtaining Pal with high purity, which allows the range of applications of this clay mineral to be expanded.

## CONCLUSIONS

Raw Palygorskite (Pal(raw)) was successfully modified by heat treatment at different temperatures seeking to remove accessory minerals that are present in this clay mineral. The heat treatment of raw Pal led to the removal of zeolite water molecules at temperatures below 150 °C and the removal of coordination water molecules between temperatures from 200 °C to 550 °C. The folding of the clay structure characterized by the removal of at least 50% of the coordination water occurred in the temperature range between 300 °C to 500 °C. Upon heat treatment, Pal exhibits good hygroscopic ability at temperatures where only zeolite water and surface-adsorbed water are lost. This is evidenced by the similar mass loss presented in the TGA between Pal(raw) and Pal(100) within the temperature range from 60-150 °C. However, when the structure is distorted due to the loss of coordination water, Pal presents a reduction in its hygroscopic capacity. The continuous removal of coordination water observed in Pal(500) and Pal(700) resulted in a decrease in surface area to values of 77 $m^2/g$ and 65 $m^2/g$, respectively. With the complete elimination of the coordination water, the clay was transformed into its anhydride state, losing its hygroscopic capacity. The dehydroxylation process occurred simultaneously with the calcite and dolomite decomposition processes, being completed in the temperature range between 700 °C and 800 °C. The full dehydroxylation of clay resulted in a decrease in surface area to 10 $m^2/g$, making it an unfavorable heat treatment for clay. Heat treatment between 100ºC and 700ºC is indicated for Pal activation, as from 100 to 300ºC the surface area of Pal is maintained at its highest values. From 500 to 700ºC there is a loss of Pal's hygroscopic ability, and its structure is maintained. At temperatures above 700ºC, changes occur in the Pal crystalline structure, which is no longer recommended, depending on the application. The results of the Pal purification process by heat treatment are promising, and they can be used for various applications after this treatment. Furthermore, the Pal purification process by heat treatment has the advantage of not generating residue, unlike what occurs in chemical treatment. The choice of treatment to be used in the purification of Pal (acid or thermal) will depend on its application.

## ACKNOWLEDGMENTS

The authors are grateful to CNPq (Conselho Nacional de Desenvolvimento Científico e Tecnológico, process 310196/2018-3) and CAPES for the financial support. This study was financed in part by the Coordenação de Aperfeiçoamento de Pessoal de Nível Superior - Brasil (CAPES) - Finance Code 001.

## REFERENCES

[1] Xavier KCM, Silva Filho EC, Santos MSF, Santos MRMC, Luz AD. Caracterização mineralógica, morfológica e de superfície da atapulgita de Guadalupe-PI, Holos 2012; **1**(5): 60-70. ISSN: 1518-1634.

[2] Bradley, W. The structural scheme of attapulgite. Am. Min.: Journal of Earth and Planetary Materials, 1940; **25**(6), 405-410.

[3] Cao L, Xie W, Cui H, Xiong Z, Tang Y, Zhang X, Feng Y. Fibrous clays in dermopharmaceutical and cosmetic applications: traditional and emerging perspectives. Int. J. Pharm., 2022; **1**(625):122097. doi:10.1016/j.ijpharm.2022.122097

[4] Wang W, Wang A. Palygorskite nanomaterials: structure, properties, and functional applications. In Nanomaterials from Clay Minerals. 2019; **1**(1):21-133. doi:10.1016/B978-0-12-814533-3.00002-8.

[5] Tian G, Han G, Wang F, Liang J. Sepiolite nanomaterials: structure, properties and functional applications. In Nanomaterials from Clay Minerals. 2019;**1**(1):135-201. Elsevier. doi: 10.1016/B978-0-12-814533-3.00003-X.

[6] Li S, Mu B, Wang X, Wang A. Recent researches on natural pigments stabilized by clay minerals: A review. Dyes and Pigments. 2021; **190**(1):109322. doi:10.1016/j.dyepig.2021.109322

[7] Hajjaji M, Alami A, El Bouadili A. Removal of methylene blue from aqueous solution by fibrous clay minerals. J. Hazard. Mater. 2006; **135 (**1-3): 188-192. doi: 10.1016/j.jhazmat.2005.11.048.

[8] Ma ZL, Tsou C H, Cui X, Wu J, Lin L, Wen H, Reyes de Guzman M, Wang C.-Y., Liu H., Xiong Q., Liao B.
Barrier properties of nanocomposites from high-density polyethylene reinforced with natural attapulgite. CRGSC. 2022;**5**(1):100314. doi:10.1016/j.crgsc.2022.100314

[9] Singer A, Huertos EG. Developments in Palygorskite-sepiolite Research: A new outlook on these nanomaterials. Elsevier. (Eds.), 2011;**1**(3):520. Paperback ISBN: 9780444536075; eBook ISBN: 9780444536082.

[10] Bergaya F, Theng BKG, Lagaly G. Handbook of Clay Science. Elsevier Science, 2006;**1**(1):1246. Paperback ISBN: 9780080971933; eBook ISBN: 9780080457635.

[11] Souza GD, Silva TF da, Albers APF, Quinteiro E, Passador FR. Purification of raw palygorskite: a comparative study involving different processes and dispersing agents. Cerâmica, 2021;**67**(382):131-138. doi:10.1590/0366-69132021673823030

[12] Habibi A, Belaroui LS, Bengueddach A, Galindo AL, Díaz CIS, Peña A. Adsorption of metronidazole and spiramycin by an Algerian palygorskite. Effect of modification with tin. Microporous and Mesoporous Materials. 2018; **268**(1): 293-

302. doi:10.1016/j.micromeso.2018.04.020
[13] Ouali A, Belaroui LS, Bengueddach A, Galindo AL, Peña A. Fe2O3–palygorskite nanoparticles, efficient adsorbates for pesticide removal. Appl. Clay Sci. 2015;**115**(1), 67-75. doi:10.1016/j.clay.2015.07.026.
[14] Barrios MS, González LF, Rodríguez MV, Pozas JM. Acid activation of a palygorskite with HCl: Development of physico-chemical, textural and surface properties. Appl. Clay Sci. 1995;**10**(3):247-258. doi:10.1016/0169-1317(95)00007-Q
[15] Neto JP, Almeida SLMD, Carvalho RDM. Atapulgita do Piauí para a indústria farmacêutica. in "Tecnologia mineral", CETEM, Brazil 1993;**63**(1). ISSN: O103-7382
[16] Boudriche L, Calvet R, Hamdi B, Balard H. Effect of acid treatment on surface properties evolution of attapulgite clay: An application of inverse gas chromatography. Balard, Colloids Surf. A Physicochem. Eng. Asp. 2011;**392**(1):45-54. doi:10.1016/j.colsurfa.2011.09.031.
[17] Theng, B.K.G. Clay Mineral Catalysis of Organic Reactions. CRC Press, 2018; 1(1):440. Paperback ISBN: 9781498746526; eBook ISBN: 9780429465789[18] Frost RL, Ding Z. Controlled rate thermal analysis and differential scanning calorimetry of sepiolites and palygorskites. Thermochim. Acta 2003;**397**(1): 119-128. doi:10.1016/S0040-6031(02)00228-9
[19] Boudriche L, Calvet R, Hamdi B, Balard H. Surface properties evolution of attapulgite by IGC analysis as a function of thermal treatment. Colloids Surf., A, 2012;**399** (1): 1-10. doi:10.1016/j.colsurfa.2012.02.015
[20] Yan W, Liu D, Tan D, Yuan P, Chen M FTIR spectroscopy study of the structure changes of palygorskite under heating. Spectrochim Acta A Mol Biomol Spectrosc. 2012; **97**(1):1052-1057. doi: 10.1016/j.saa.2012.07.085
[21] Kulbicki G. High temperature phases in sepiolite, attapulgite and saponite. Am Min. 1959; **44**(1):752-764.
[22] Preisinger A Sepiolite and related compounds: its stability and application. Clays and Clay Minerals 1961; **10**(1): 365-371. doi:10.1346/CCMN.1961.0100132
[23] Ahlrichs JL, Serna C, Serratosa JM. Structural hydroxyls in sepiolites. Clays and Clay Minerals 1975:**23**(5):119-124. doi: 10.1346/CCMN.1975.0230207
[24] Krekeler M P, Guggenheim S. Defects in microstructure in palygorskite–sepiolite minerals: A transmission electron microscopy (TEM) study. Appl. Clay Sci. 2008; **39**(1): 98-105. doi:10.1016/j.clay.2007.05.001
[25] Kuang W, Facey GA, Detellier C. Dehydration and rehydration of palygorskite and the influence of water on the nanopores. Clays and Clay Minerals 2004;**52** (5): 635-642. doi:10.1346/CCMN.2004.0520509
[26] Balci S. Effect of heating and acid pre-treatment on pore size distribution of sepiolite. Clay Miner. 1999;**34**(4): 647-655. doi: 10.1180/000985599546406
[27] Liu X, Liu X, Hu Y. Investigation of the thermal behaviour and decomposition kinetics of kaolinite. Clay Miner. 2015; **50**(2):199-209. doi: 10.1180/claymin.2015.050.2.04
[28] Karunadasa KS, Manoratne CH, Pitawala HMTGA, Rajapakse RMG. Thermal decomposition of calcium carbonate (calcite polymorph) as examined by in-situ high-temperature X-ray powder diffraction. Thermal decomposition of calcium carbonate (calcite polymorph) as examined by in-situ high-temperature X-ray powder diffraction. Journal of Physics and Chemistry of Solids, 2019;**134**(1029):21-28. doi:10.1016/j.jpcs.2019.05.023
[29] Olszak-Humienik M, Jablonski M. Thermal behavior of natural dolomite. J. Therm. Anal. Calorim. 2015;**119**(12): 2239-2248. doi: 10.1007/s10973-014-4301-6
[30] Zhou X, Liu D, Bu H, Deng L, Liu H, Yuan P, Du P, Song H. XRD-based quantitative analysis of clay minerals using reference intensity ratios, mineral intensity factors, Rietveld, and full pattern summation methods: A critical review. Solid Earth Sciences, 2018; 3(1), 16-29. doi: 10.1016/j.sesci.2017.12.002
[31] Bergaya F, Jaber M, Lambert JF. Clays and clay minerals. Appl. Clay Sci. 2011; **19**(1): 1-3.
[32] Silva TF da, Albers A.P.F., Quinteiro E., Sundararaj U., Passador F.R. Mechanical, thermal, rheological, and morphological characterization of polyolefin/activated attapulgite nanocomposites. J. Appl. Polym. Sci., 2023; **140**(39): e54471. doi: 10.1002/app.54471.
[33] VanScoyoc GE, Serna CJ, Ahlrichs JL. Structural changes in palygorskite during dehydration and dehydroxylation. Am. Min. 1979; **64**(1):215-223. doi:0003-004x/79/0 102_02 15$02.09
[34] Lynwood HW, Schwint IA. Attapulgite, its properties and application. Ind. Eng. Chem. 1967;**59**(9); 58–69. doi: 10.1021/ie51403a012
[35] Barrer RM. Mackenzie N. Sorption by attapulgite. I. Availability of intracrystalline channels. J. Phys. Chem. 1954;**58**(7): 560-568. doi:10.1021/j150517a013
[36] Silva T F da, Souza GPM de, Morgado GF de M, Wearn YN, Albers APF, Quinteiro E, Passador FR, A Brief Review of the Latest Advances of Attapulgite as a Reinforcing Agent in Polymer Matrix Nanocomposites. AJEAS,2012; **14**(2):292-307. doi: 10.3844/ajeassp.2021.292.307.
[37] Silva TF da, Morgado GF de M, Albers A.P.F, Quinteiro E, Passador FR, High-density polyethylene/attapulgite (ATP) nanocomposites: Effect of the organophilization of ATP on the structural, mechanical, and thermal properties. J. Appl. Polym. Sci., 2022; **139**(27): e52502. doi: 10.1002/app.52502.
[38] Silva TF da, Souza GPM de, Morgado GF de M, Albers APF, Quinteiro E, Passador FR. Influence of surface modification of attapulgite (ATP) with aminosilane (3-aminopropyl) triethoxysilane for the preparation of LLDPE/ATP nanocomposites J. Polym. Res., 2002; **29**(3): 95. doi: 10.1007/s10965-022-02953-3.
[39] Zhu J, Zhang P, Wang Y, Wen K, Su X, Zhu R, He H, Xi Y. Effect of acid activation of palygorskite on their toluene adsorption behaviors. Ap. Clay Science, 2018; **159**(1), 60–67. doi: 10.1016/j.clay.2017.07.019
[40] Chen H, Zhao J, Zhong A, Jin Y. Removal capacity and adsorption mechanism of heat-treated palygorskite clay for methylene blue. Chemical Engineering Journal - Chem Eng J, 2011, **174**(10), 143–150. doi:10.1016/j.

cej.2011.08.062.
*(Rec. 15-Apr-2024, Rev. 05-Aug-2024, Rev. 04-Oct-2024, Ac. 09-Oct-2024)*
*(AE: A. M. Segadães)*